

Moderate Constant Power Properties of Series Resonant Networks

Shmuel (Sam) Ben-Yaakov, *Life Fellow, IEEE*
 Department of Electrical and Computer Engineering
 Ben-Gurion University of the Negev
 P.O. Box 653, Beer-Sheva, 8410501 Israel
 sby@bgu.ac.il
 http://www.ee.bgu.ac.il/~pel

Abstract—This work reveals that series resonant networks (SRN) operating under CCM condition, can deliver approximately constant power under varying load condition without a frequency change or duty cycle control. The model developed in the study, delineates the relationship between characteristic impedance, the deviation of the excitation frequency from the resonant frequency, the load resistance and the output power for a given input voltage. As such, the model could be used to design a constant power SRN or a series resonant converter for a given application. Experimental and simulation results verify the analytical model developed in the study.

Keywords—series resonant, constant power, modelling, SPICE, series resonant converter.

I. INTRODUCTION

Resonant networks and their properties are basic electrical subjects that are covered in practically all electrical engineering textbooks. The importance of the series resonant network (SRN) in power electronics stems from the fact that it is the precursor of the series resonant converter (SRC) that has been found to be very useful in a wide range of applications such as induction heating, high output voltage converters, capacitor chargers, and others [1-15]. Analysis and design of the SRC is often carried out by a simplified equivalent SRN that is obtained by applying the first harmonics approximation and the Rac equivalent resistor concept [16]. Applying this and other analytical methods, the characteristics of the SRC were presented extensively in many previous publications [17-21]. Although the SRC converters possess some inherent characteristics such as a high output impedance [17], they are operated in most cases in closed loop by monitoring the output voltage, output current or output power, and a feedback loop that controls the driver's switching frequency, duty cycle or both.

This work reveals a new characteristic of the SRN that has not been explored hitherto. It is proven that under some specific operating conditions, the SRN can be operated as a power source for a relatively wide range of loads. The focus of this paper is the analysis and demonstration of the constant power capability of the SRN and it does not dwell into SRC realizations which are only discussed briefly in the 'conclusion' section.

II. THE OBSERVATION

By running a circuit simulation of an SRN (Fig. 1), one can obtain the familiar family of voltage gain curves (V_{out}/V_{in}) between the source V_{in} and the voltage across the load R , V_{out} , as function of the excitation frequency f_s (Fig. 2). Fig. 2 is plotted for a normalized SRN with input voltage, V_{in} , of 1V, resonant frequency f_o , of 1Hz and a characteristic impedance, Z , of 1Ω . As can be observed in the parametric plot of Fig. 2, none of the curves cross each other, except for the joint point at the resonant frequency. This implies that for any given excitation frequency, the gain changes as the load resistance varies. Examination of the output power (Fig. 3a) of the normalized demo circuit of Fig. 1, reveals an extensive crossing between the power curves. For example, at around 1.14Hz a number of curves cross each other as seen in the zoomed and more detailed plot (Fig. 3b). This implies that at that excitation frequency, the output power is about constant for a specific range of load resistors. This constant power attribute is explored by the model developed in this study.

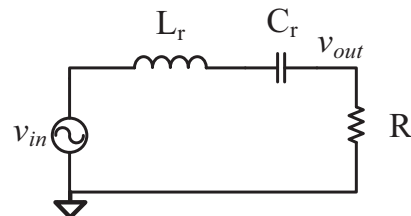


Fig. 1. The generic series resonant converter.

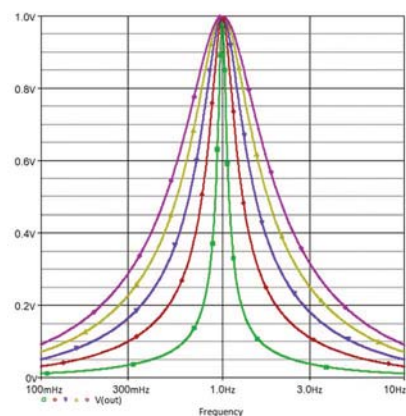
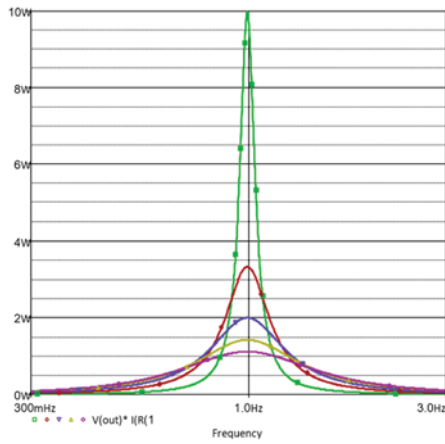
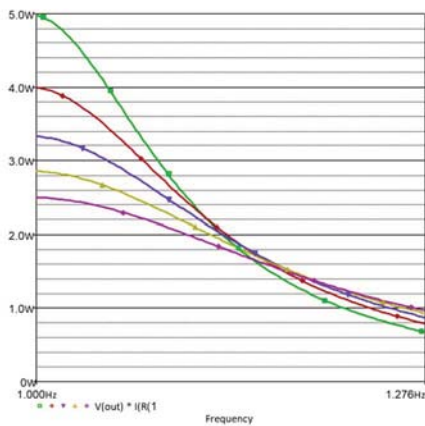


Fig. 2. Typical voltage gain ratio of a series resonant network for a range of load resistors.



(a)



(b)

Fig. 3. (a) Normalized output power of a series resonant network for a range of load resistors. (b) Zoom on a region with crossing output power curves.

III. ANALYTICAL MODEL DEVELOPMENT

The output to input voltage ratio of an SRN can be expressed as

$$\frac{V_{out}}{V_{in}}(f) = \frac{1}{\sqrt{1+Q^2\left(\frac{f_s-f_o}{f_o}\right)^2}} \quad (1)$$

where: V_{out} =Output voltage; V_{in} = Input voltage;
 $\omega_0 = \frac{1}{\sqrt{C_r L_r}}$; $\omega_0 = 2\pi f_0$; C_r = Resonant capacitor;
 L_r = Resonant inductor; f_r = Resonant frequency;
 f_s = Drive frequency;

$$Q = \frac{Z}{R} = \frac{\omega_0 L_r}{R}; Z = \sqrt{\frac{L_r}{C_r}}; R = \text{Load resistance}$$

From above, the output power, P , can be expressed as

$$P = \frac{V_{in}^2}{R\left(1+\left(\frac{\omega_0 L_r}{R}\right)^2 X^2\right)} = \frac{V_{in}^2}{R+\frac{(Z)^2}{R} X^2} = \frac{V_{in}^2}{R+\frac{Y}{R}} \quad (2)$$

$$\text{Where } Y = (Z \cdot X)^2; X = \frac{f_s}{f_o} - \frac{f_o}{f_s}$$

The normalized equation (2) ($V_{in}^2=1$; $Y=1$) is depicted in Fig. 4.

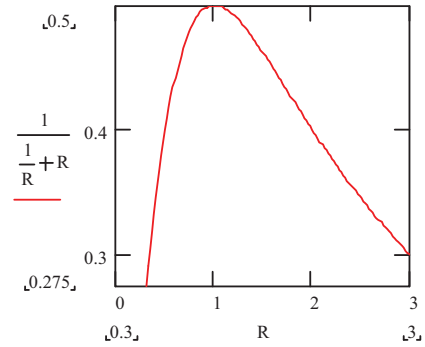


Fig. 4. Normalized output power as a function of R for $Y=1$, $V_{in}=1$ (equation 2).

As observed, equation (2) is a parabolic function reaching a maximum when

$$R_m = \sqrt{Y} = Z \cdot X \quad (3)$$

$$\text{and hence, } Y = R_m^2$$

with a maximum power value P_m of

$$P_m = \frac{V_{in}^2}{2R_m} \quad (4)$$

Since any horizontal line in Fig. 4, below 0.5, will cross the parabolic curve twice, it implies that any two load resistors will receive the same power for any given switching frequency. This explains the observed curves crossing in Figs. 3a and 3b. For a SRN with a given V_{in} and Y , the resistances of the two resistors R_1 , R_2 , that will receive the same power P are

$$R_1, R_2 = \frac{\frac{V_{in}^2}{P} \pm \sqrt{\frac{V_{in}^4}{P^2} - 4Y}}{2} \quad (5)$$

which converges to a single value R_m at P_m .

The relationship between the relative load resistance variation, K , and relative power change, P_r , can be expressed as:

$$P_r = \frac{P(KR_m)}{P(R_m)} = \frac{\left(\frac{V_{in}^2}{KR_m + \frac{R_m^2}{KR_m}}\right)}{\frac{V_{in}^2}{2R_m}} = \frac{2}{K + \frac{1}{K}} \quad (6)$$

where $K = R/R_m$.

This relationship is depicted Fig. 5 which delineates the constant power capabilities of the SRN. For example for a 50% change of the load resistance the output power will change by 10% $\{2/(1.5+1/1.5)=0.9\}$.

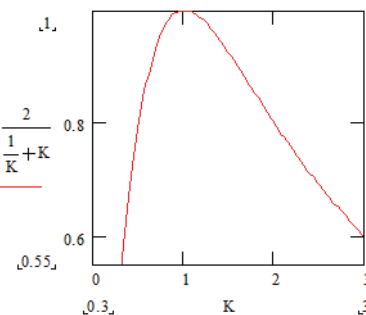


Fig. 5 Relative change in power as a function of relative change in load resistance (equation 6).

From

$$P_m = \frac{V_{in}^2}{2R_m} = \frac{V_{om}^2}{R_m} \quad (7)$$

the maximum output voltage, V_{om} , at maximum power, P_m , is found to be:

$$V_{om} = \frac{V_{in}}{\sqrt{2}} \quad (8)$$

The output current I_o can be expressed as

$$I_o = I_{om} \sqrt{\left(2 - \frac{V_o^2}{V_{om}^2}\right)} \quad (9)$$

where the maximum output current, I_{om} , is

$$I_{om} = \sqrt{\frac{P_m}{R_m}} \quad (10)$$

Equation (9) is highly relevant to capacitor charging since it shows how the current is changing as the capacitor is charged. The function $I_n = I_o/I_{om} = f(V_o/V_{om})$ is depicted in Fig. 6.

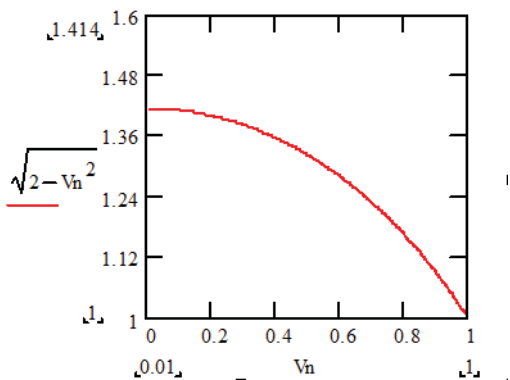


Fig. 6. Normalized output current I_n ($I_n = I_o/I_{om}$), vertical axis, as a function of the normalized output voltage ($V_n = V_o/V_{om}$) - per equation (9).

From (9), the power delivered to the load as a function of the load voltage can now be expressed as

$$P_o = P_{om} \frac{V_o}{V_{om}} \sqrt{\left(2 - \frac{V_o^2}{V_{om}^2}\right)} \quad (11)$$

The normalized behavior of this function is depicted in Fig. 7.

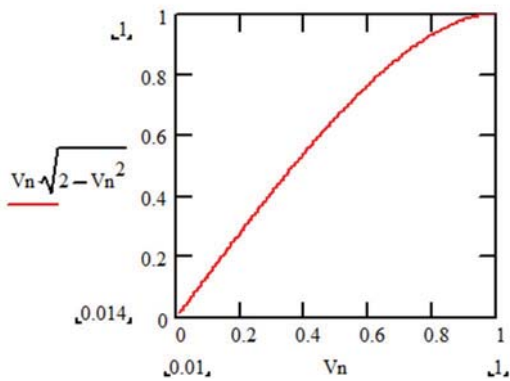


Fig. 7. Normalized output P_n ($P_n = P_o/P_{om}$), vertical axis, as a function of the normalized output voltage ($V_n = V_o/V_{om}$) - per equation (11)

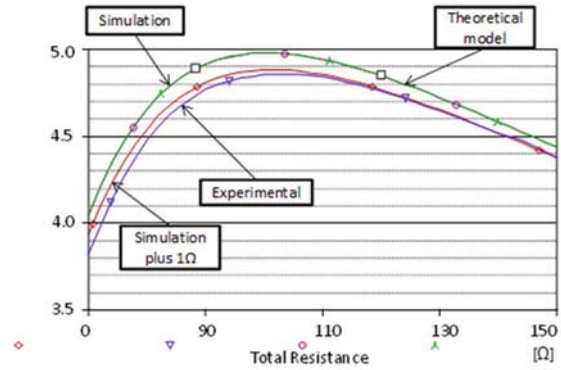


Fig. 8. Comparison of experimental, simulation and model calculation results. “Simulation plus 1Ω” accounts for parasitic resistance in experimental set up.

IV. EXPERIMENTAL

Experiments were carried out on the basic resonant network (Fig. 1) having the following parameters: $L_r = 47\mu\text{H}$, $C_r = 0.22\mu\text{F}$, Drive frequency = 61.2kHz, Drive amplitude = 5Vpp. Source resistance: 50Ω. The series load resistor (in addition to source resistance) was changed between 20Ω and 100Ω in increments of 5Ω. Excellent agreement was found between experimental, simulation and model calculation results. Simulation was repeated (“Simulation plus 1Ω”) to include the parasitic resistance that was apparently present in the experimental set up. This improved the matching of the experimental and simulation results.

IV. DISCUSSION AND CONCLUSIONS

This work reveals that series resonant networks (SRN) operating under CCM condition, can deliver approximately constant power under varying load condition without a frequency change or duty cycle control. The model developed in the study, delineates the relationship between characteristic impedance, Z , the deviation of the switching frequency from the resonant frequency X , the load resistance and the output power for a given input voltage. As such it could be used to design a SRN or a SRC for a given application.

The presented model explains the fact that any two load resistors will receive the same power at one specific switching frequency predicted by the model. This explains the observed crossing of the curves in Fig. 3a and 3b. The implication of this crossing is that load with resistances in the neighborhood of R_m , will receive approximately the same power, the degree of which is expressed by (6) and depicted in Fig. 4. A corollary of the model which agrees with earlier publication [17] is that the output current of the SRN as a function of the output voltage, for a fixed switching frequency, changes by only about 40% from zero voltage to the voltage of maximum power. This exhibits the current sourcing nature of the SRN which is the precursor of the SRC. However, despite the increase in current at low output voltage (Fig. 5), the power level drops considerably at low output voltages (Fig. 6).

The implications of this study are that when the variations of the load resistance of the SRN are moderate it will deliver approximately constant power. For example, for a 30% change in load resistance the power variation will be only about -3.5%. However, in the case of large output voltage variations, such as in the case of a capacitor charging by a fixed switching frequency CCM SRC, the SRN behaves more like a current source and hence the power delivered at the initial voltage range will be relatively low (Fig. 6). This behavior conforms with good engineering practice since constant power charging at the low voltage range implies unacceptable charging current.

Based on the above, it can be concluded that the contribution of the analytical model developed in this work is the added insight into the behavior of the CCM operated SRN and hence the SRC.

REFERENCES

- [1] S. D. Johnson, A. F. Witulski, and R. W. Erickson, "Comparison of Resonant Topologies in High Voltage Applications," *IEEE Transactions on Aerospace and Electronic Systems*, vol. 24, no. 3, pp. 263-274, May 1988.
- [2] Chan-Hun Yu, S. R. Jang, Hyoung-Suk Kim, Gideon Nimo Appiah and H. J. Ryoo, "Design of a high efficiency 40kV, 300us, 200Hz solid-state pulsed power modulator with long pulse width," *IECON 2016 - 42nd Annual Conference of the IEEE Industrial Electronics Society*, Florence, 2016, pp. 3342-3347.
- [3] A. Namadmalan, "Universal Tuning System for Series-Resonant Induction Heating Applications," in *IEEE Transactions on Industrial Electronics*, vol. 64, no. 4, pp. 2801-2808, April 2017.
- [4] Y. Baskurt and H. Karaca, "Design and Realization of a 100 kHz - 100 kW Series Resonant Inverter with SiC-MOSFETs Connected in Parallel for a High Frequency Induction Heating," *PCIM Europe 2017; International Exhibition and Conference for Power Electronics, Intelligent Motion, Renewable Energy and Energy Management*, Nuremberg, Germany, 2017, pp. 1-6.
- [5] M. H. Cheng and T. J. Liang, "An atmospheric pressure plasma power supply with digital constant power control," *2013 1st International Future Energy Electronics Conference (IFEEEC)*, Tainan, 2013, pp. 332-337.
- [6] B. Ni, C. Y. Chung and H. L. Chan, "Design and comparison of parallel and series resonant topology in wireless power transfer," *2013 IEEE 8th Conference on Industrial Electronics and Applications (ICIEA)*, Melbourne, VIC, 2013, pp. 1832-1837.
- [7] V. K. S. Veeramallu, S. Porpandiselvi and B. L. Narasimharaju, "Reduced ripple current LED lighting system with two series resonant converters," *2017 2nd International Conference on Communication and Electronics Systems (ICCES)*, Coimbatore, 2017, pp. 1025-1030.
- [8] K. Tomas-Manez, Z. Zhang and Z. Ouyang, "Unregulated series resonant converter for interlinking DC nanogrids," *2017 IEEE 12th International Conference on Power Electronics and Drive Systems (PEDS)*, Honolulu, HI, 2017, pp. 647-654.
- [9] B. Y. Luan, S. Hu, Y. F. Zhang and X. Li, "Steady-state analysis of a series resonant converter with modified PWM control," *2017 12th IEEE Conference on Industrial Electronics and Applications (ICIEA)*, Siem Reap, 2017, pp. 1143-1148.
- [10] M. Salem, A. Jusoh, N. R. N. Idris, C. W. Tan and I. Alhamrouni, "Phase-shifted series resonant DC-DC converter for wide load variations using variable frequency control," *2017 IEEE Conference on Energy Conversion (CENCON)*, Kuala Lumpur, 2017, pp. 329-333.
- [11] S. Hu, X. Li and A. K. S. Bhat, "Operation of a bidirectional series resonant converter with minimized tank current and wide ZVS range," in *IEEE Transactions on Power Electronics*.
- [12] Q. Zhu, L. Wang, A. Huang, K. Booth and L. Zhang, "7.2 kV Single Stage Solid State Transformer Based on Current Fed Series Resonant Converter and 15 kV SiC MOSFETs," in *IEEE Transactions on Power Electronics*.
- [13] T. N. Gucin, B. Fincan and M. Biberoglu, "A Series Resonant Converter Based Multi Channel LED Driver with Inherent Current Balancing and Dimming Capability," in *IEEE Transactions on Power Electronics*.
- [14] B.S. Nathan, V. Ramanarayanan, "Analysis simulation and design of series resonant converter for high voltage applications," *Industrial Technology 2000. Proceedings of IEEE International Conference on*, vol. 1, pp. 688-693 vol.2, 2000.
- [15] Ji-Woong Gong, S. H. Ahn, H. J. Ryoo and S. R. Jang, "Comparison of DCM and CCM operated resonant converters for high-voltage capacitor charger," *IECON 2013 - 39th Annual Conference of the IEEE Industrial Electronics Society*, Vienna, 2013, pp. 532-537
- [16] R. L. Steigerwald, "A comparison of half-bridge resonant converter topologies," in *The 2nd IEEE Applied Power Electronics Conference and Exposition*, 1987, pp. 135-144.
- [17] A. Witulski and R. Erickson, "Steady-State Analysis of the Series Resonant Converter," *IEEE Transactions on Aerospace and Electronic Systems*, vol. AES-21, no. 6, pp. 791-799, November 1985.
- [18] S. Trabert and R. Erickson, "Steady-State Analysis of the Duty-Cycle Controlled Series Resonant Converter," *IEEE Power Electronics Specialists Conference*, 1987 Record, pp. 545-556.
- [19] Arthur F. Witulski and Robert W. Erickson, "Small Signal AC Equivalent Circuit Modelling of the Series Resonant Converter," *IEEE Power Electronics Specialists Conference*, 1987 Record, pp. 693-704.
- [20] M.K. Kazimierczuk, S. Wang, "Frequency-domain analysis of series resonant converter for continuous conduction mode", *Power Electronics IEEE Transactions on*, vol. 7, pp. 270-279, 1992, ISSN 0885-8993.
- [21] R. L. Steigerwald, "A comparison of half-bridge resonant converter topologies," in *The 2nd IEEE Applied Power Electronics Conference and Exposition*, 1987, pp. 135-144.